Uranium (VI) reduction in a fixed-film reactor by a bacterial consortium isolated from uranium mining tailing heaps

Phalazane J. Mtimunye and Evans M.N. Chirwa

Water Utilisation and Environmental Engineering Division, Department of Chemical Engineering, University of Pretoria, Pretoria, 0002, South Africa

*Corresponding author.
Water Utilisation and Environmental Engineering Division, Department of Chemical Engineering, University of Pretoria, Pretoria, 0002, South Africa
Evans.Chirwa@up.ac.za

Highlights

• A locally isolated mixed-culture of bacteria reduced U^{6+} in a fixed-film bioreactor.

• Fixed-film bioreactor achieved higher U(VI) removal without bio-stimulation.

• Fixed-film bioreactor system proved robust by stabilize high U(VI) loading rates.

• SEM, XRD and TEM showed U^{4+} deposits on surface thus U^{6+} reduction is extracellular.

• Extracellular U^{6+} reductase activity shows feasibility of easy recovery of uranium.

Abstract

Biological uranium (VI) reduction was investigated using a mixed-culture of U(VI) reducing bacteria isolated from tailing dumps at an abandoned uranium mine in Pharaborwa (Limpopo Province, South Africa). A fixed-film reactor was used in the investigation, whereby the reactor was operated in the up-flow mode under fully submerged conditions at a recirculation ratio of, $Q_{in}/Q_R = 20$. The performance of the bioreactor was evaluated over a range of influent U(VI) concentrations [75–100 mg U(VI)/L] and 24 h hydraulic retention time [HRT]. Complete U(VI) removal was observed in phases with 30–85 mg/L influent U(VI). When influent U(VI) was increased to 100 mg/L, approximately 60% U(VI) removal was achieved. The oxidation states of reduced uranium species were determined by Scanning and Transmission Electron Microscopy followed by X-ray Diffractometer (SEM/TEM-XRD). Earlier studies in batch systems showed that U(VI) was non-toxic to U(VI) reducing organisms at concentrations up to 400 mg/L. The decrease in U(VI) removal efficiency observed in the fixed-film reactor after 42 days was therefore attributed to the accumulation of U(IV) hydroxide precipitates in the reactor. Genetic identification using the 16S rRNA gene sequence analysis showed that the species *Kocuria turfanensis, Arthrobacter creatinolyticus, Bacillus licheniformis,* and *Microbacterium aerolatum* survived from the original cultures. The feasibility of continuous removal of U(VI) in an inoculated indigenous culture system was thus demonstrated.

Keywords

U(VI) reduction; U(VI) reductase; Biofilm; 16S rRNA; Uranium species; Mass transfer resistance

Graphical abstract

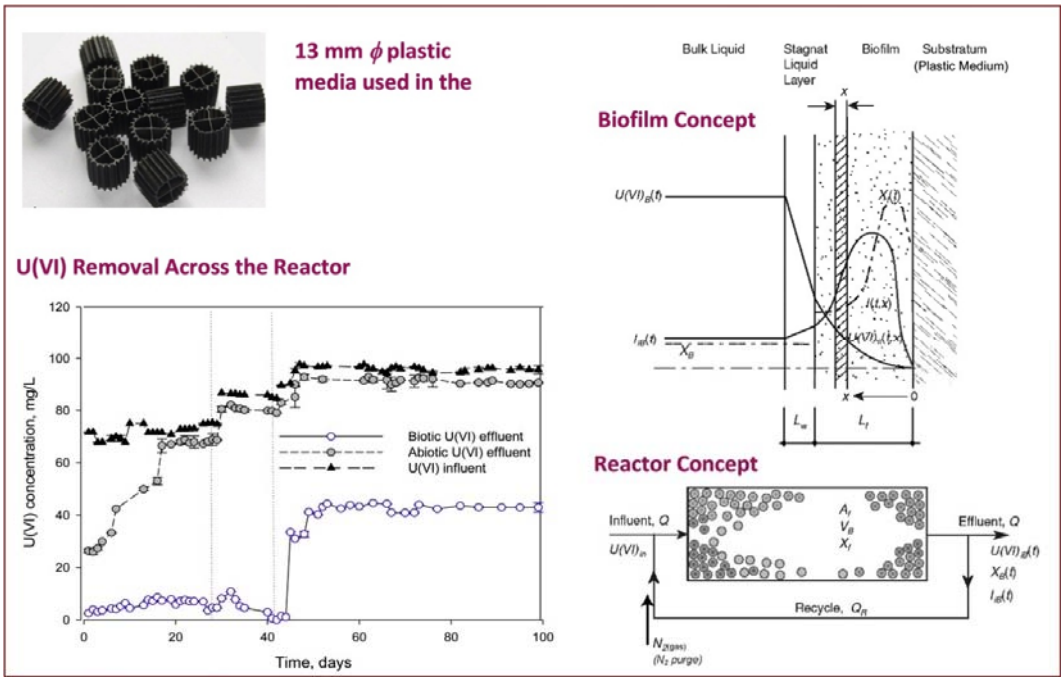

1. Introduction

1.1. Background

Uranium is known to be the heaviest naturally occurring and potentially fissionable element in nature since its discovery by mineral chemist Martin Heinrich Klaproth [1]. Occurrence of fissionable natural uranium is ubiquitous on earth where evidence points to levels higher than 3% U-235 at some point in time. In one specific case, it is suggested that nuclear decomposition of a geological formation containing high levels of U-235 collapsed resulting in the release of a large amount of neutrons that sustained a chain reaction for 1.5 million years or longer in Gabon (West Africa) [2]. In order to sustain the chain reaction for such a long time, the neutron flow was regulated by the variations in the water level in the groundwater aquifer below it. Otto Hahn [3] verified the ability of U-235 to fission into smaller components with the resultant release of free neutrons and an enormous amounts of energy. Since its discovery, the potential of uranium as a source of friendly nuclear energy was highlighted even by early researchers whose focus was in the development of weapons grade fissionable materials [4,5]. In the natural environment, uranium exists as an inorganic complex in the oxides of uranium, i.e., uraninite (UO_2), uranium trioxide (UO_3), and triuranium octaoxide

(U_3O_8) also known as pitchblende [6]. Among the listed species, U_3O_8 is the most thermodynamically stable. U_3O_8 is used in various commercial applications such as colouring reagents, glazing pigmentation, nuclear power generation, radioisotope manufacturing, and biomedical research [7].

For many years, uranium destined for commercial use was leached from natural rock deposits using alkaline or acid leaching solutions such as sulfuric acid, nitric acid, ammonia, and carbonate containing solutions [8]. This method of uranium extraction from natural rocks was later prohibited due to a range of political, economic, and environmental reasons. Today, underground mining of uranium ore for commercial purposes remains the most preferred method for extracting uranium from natural rocks. During the process of uranium mining and concentration using conventional methods, environmental impacts are often ignored. Uranium used in electricity generation in nuclear reactors is generally sourced from ores with uranium oxide concentrations up to 10%. However, lower grade ores with uranium oxide concentration of 0.2% or less are the most common and the most mined [9,10]. The uranium concentrate used in nuclear reactors is typically at 75–95% uranium oxide (U_3O_8). Mining of such readily available lower grade uranium ore to achieve about 75–95% U_3O_8 concentrate used in nuclear power plants results in the release of large amounts of waste rock tailings with significant environmental consequences due the presence of residual uranium in the rocks [10].

Uranium in tailing dumps exists either as U(VI) or U(IV) depending on the pH and redox conditions at the site. However, it is preferable to keep uranium in the dump sites in the tetravalent form [U(IV)] and not in the hexavalent state U(VI). This is because, unlike U(VI) which is highly toxic and mobile in aquatic environments, U(IV) precipitates easily as $U(OH)_4(s)$ and is entrapped in the medium thereby preventing long range pollution. Upon reaching the environment, U(VI) may be easily taken up by plants and other life-forms including humans [11]. Uptake of uranium at concentrations ranging from about 50 to 150 mg/kg causes complications such as acute liver or kidney failure and even death [12,13]. Because uranium is known to be both radiotoxic and bioaccumulative, multidisciplinary studies have been undertaken to evaluate its long-term impacts on the environment [11,14].

Initial efforts at reducing U(VI) using bacteria were conducted in anaerobic batch reactors culture isolates from soil [[15], [16], [17]]. The batch studies were used to derive reaction rate laws and to obtain parameters to be used later in continuous flow processes [17]. Typically, treatment of large volumes of wastewater coming

from power generation plants in batch systems could be difficult. In this study, the biofilm reactor system is proposed both as a scalable continuous flow process that can be used to handle large flows and to maximise the retention of biomass which is the main catalysis for the U(VI) reduction process. Additionally, from the continuously operated system, dynamic parameters such as diffusion, dispersion and flow regimes are obtained. Results from such a system may be sufficient to understand kinetic processes taking place in the complex system with respect to reaction and hydrodynamic properties.

Biofilm systems are preferred over suspended growth systems due their high surface area for reaction, long cell retention times, and resilience against toxicity [18]. The heterogeneous nature of the biofilm structure allows for nutrient recycling and creation of diverse ecosystems within the biofilm, which is conducive to the formation of complex pathways required for the breakdown or bioconversion of most toxic recalcitrant pollutants.

1.2. Kinetic model derivation

To model a biological U(VI) reducing system, the reaction scheme, rate equations, and kinetic constants for the processes taking place in the batch reactor are chosen from published models on enzymatic reduction hexavalent toxic metals [[19], [20], [21], [22], [23]]. Biochemical studies on U(VI) reduction suggested that U(VI) reducing mechanisms may be coupled to the membrane-electron transport system in U(VI) reducing bacteria and the rate of U(VI) reduction catalyzed by enzymes can be expressed as follows:

$$U(VI)+E \underset{k2}{\overset{k1}{\rightleftarrows}} E*U(VI) \xrightarrow{k3} E+U(IV) \tag{1}$$

where: E = enzyme, E*U(VI) = enzyme-U(VI) complex, k_1 = rate constant for complex formulation, k_2 = rate constant for reverse complex formulation, k_3 = rate constant for U(IV) formation.

Let U(VI) = U and E^*U(VI) = E^* (2)

The rate laws of formation of E^* in (Eq. (2)) result in the following equation:

$$\frac{dE^*}{dt} = k_1 U(E-E^*) - k_2 E^* - k_3 E^* \tag{3}$$

E* is the representative enzyme that is logically proportional to viable cell concentration X is the only metabolic component in the culture. E^* can either be formed or destroyed such that $\frac{dE^*}{dt}$ is approximately zero, thus $\frac{dE}{dt} \approx 0$.

Consequently, the mass balance represented in (Eq. (4)) can be expressed in terms of the active enzyme E as follows:

$$E^* = \frac{k_1 UE}{k_1 U + k_2 + k_3} - \frac{UE}{U + \frac{k_2 + k_1}{k_1}} \quad (4)$$

Then U(VI) reduction rate in (Eq. (4)) can be expressed as:

$$\frac{-dU}{dt} = \frac{k_3 UE}{U + \frac{k_2 + k_3}{k_1}} \quad (4)$$

Analogous to Monod kinetics [24], k_3 is analogous to maximum specific U(VI) reduction rate (k_u), E is analogous to biomass concentration (X) and $\frac{k_2+k_3}{k_1}$ is analogous to half-velocity concentration (K_u) [25].

$$\frac{-dU}{dt} = \frac{k_u \cdot U}{K_u + U} \cdot X \quad (5)$$

where: U = U(VI) concentration at time, t (mg/L); X = concentration of active bacterial cells at time, t (mg cells/L); k_u = specific rate of U(VI) reduction (mg U(VI)/mg cells/h); and K_u = half-saturation coefficient (mg/L).

1.3. Reactor mass balance derivation

1.3.1. Advection

The transport of dissolved U(VI) species from one point to another governed by bulk motion of fluid as follows:

$$\frac{-dU_B}{dt} V_B = Q(U_{in} - U_B) \quad (6)$$

where: U_B = U(VI) concentration at the bulk liquid zone at time, t (ML^{-3}), V_B = bulk liquid volume (L^3), U_{in} = influent U(VI) concentration (ML^{-3}), Q = influent flow rate (L^3T^{-1}), and t = time (T).

1.3.2. Molecular diffusion

The transport of all dissolved species across the boundary layer (L_w) into the biofilm is caused by random molecular motions and collusions of particles themselves. Molecular diffusion is the only means of mass transport mechanism within the biofilm that follows Fick's law and can be defined as a function of external mass transfer resistance (K_{LU}) across the surface area and bulk U(VI) concentration as follows:

$$\frac{-dU_B}{dt} V_B = K_{LU} A_f (U_B - U_{sf}) = \frac{D_{uw}}{L_w} A_f (U_B - U_s f) = j_u A_f \quad (7)$$

where: A_f = total biofilm surface area (L^2), D_{uw} = diffusion coefficient of dissolved uranium species in water (L^2T^{-1}), L_w = the thickness of the stagnant liquid layer, which may decrease the flux of dissolved particles into the biofilm (L), U_B = U(VI) concentration at the bulk zone at time, t (ML^{-3}), U_{sf} = liquid-biofilm interface U(VI) concentration (ML^{-3}). In most mass transfer limited reactions $U_B << U_{sf}$, thus U_{sf} is negligible and may therefore be omitted in the equation above. The external mass transfer resistance, K_{LU}, (LT^{-1}) can be visualized by introducing a boundary layer (L_w) as follows:

$$K_{LU} = \frac{D_{uw}}{L_w} \tag{8}$$

1.3.3. Adsorption

The rate at which U(VI) is removed across the reactor is dependent on the rate at which U(VI) is transported across the liquid layer by diffusion and adsorbed within the biofilm matrix. The rate at which U(VI) can be reduced on the surface area of the biofilm is defines as:

$$\frac{-dU_B}{dt} = k_{ad}(U_{eq} - U_B) = q_u \tag{9}$$

where: k_{ad} = U(VI) adsorption rate coefficient (T^{-1}), U_{eq}= equilibrium bulk liquid U(VI) concentration (ML^{-3}), U_{sf} = liquid-biofilm interface U(VI) concentration (ML^{-3}).

1.3.4. Microbial reduction

The rate of U(VI) reduction in the biological system is highly dependent on the number of active cells present in the reactor, and the capacity of cells to produce enzymes that can reduce U(VI) under various loading concentrations. A fraction of cells leaving the biofilm and exiting the reactor after time equivalent to HRT of the reactor are assumed to be at resting conditions. It has been shown in batch kinetic studies that resting cells may reduce U(VI) without the accompanying cell growth. It is suggested therefore that the amount of U(VI) reduced under resting cells conditions will be proportional to the amount of cells inactivated by U(VI) (Nkhalambayausi-Chirwa and Wang, 2005) [26].

The inhibitory effects observed in the reactor over time at higher initial U(VI) concentration of 100 mg/L under oxygen stressed conditions suggested incorporation of U(VI) toxicity threshold concentration, U_r, and deactivation coefficient of cells in the system. Therefore, a mathematical model incorporating U(VI) toxicity threshold concentration, U_r, and deactivation coefficient of cells in the system was used during simulation of U(VI) effluent concentration:

$$\frac{-dU_B}{dt} = \frac{k_u U_B}{K_u + U_B\left(K^{\left(1-\frac{U_B}{U_r}\right)}\right)}\left(X_B - \frac{U_{in}-U_B}{T_u X_B}\right) = r_{uB} \quad (10)$$

where: k_u= specific rate of U(VI) reduction ($L^3M^{-1}T^{-1}$), K_u = half-velocity coefficient (ML^{-3}), X_{oB} = initial cell concentration at the bulk zone (ML^{-3}), U_{in} = influent U(VI) concentration (ML^{-3}), K = dimensionless U(VI) inhibition factor, U_r = inhibition threshold concentration (ML^{-3}), T_u= maximum U(VI) reduction capacity of cells [g U(VI) reduced/g cells] (MM^{-1})].

The overall non-linier equations from Eqs. (1) to (10) governing the liquid phase at transient state yield the following mass balance equation of the dissolved species across the bulk liquid zone of the reactor:

$$\frac{dU_B}{dt}V_B = Q(U_{in} - U_B) - r_u BV_B - q_u V_B - j_u A_f \quad (11)$$

where: U_B = U(VI) concentration at the bulk liquid zone at time, t (ML^{-3}), V_B = bulk liquid volume (L^3), U_{in} = influent U(VI) concentration (ML^{-3}), Q = influent flow rate (L^3T^{-1}), r_{uB}=U(VI) reduction rate coefficient at the bulk phase ($ML^{-3}T^{-1}$), q_u= rate of U(VI) removal by adsorption (T^{-1}), j_u= U(VI) flux rate (ML^2T^{-1}), A_f = surface area in the biofilm reactor (L^2), t = time (T), and r_u = dissolved species removal rate ($ML^{-3}T^{-1}$),

The terms $\boldsymbol{q_u}$,$\boldsymbol{j_u}$, $\boldsymbol{r_u}$ in the above equations represent adsorption, diffusion processes, and reaction by suspended or inert cells in the bulk liquid respectively. The term $\boldsymbol{q_u}$ in the above equation can approach equilibrium easily whereas the terms $\boldsymbol{r_u}$ and $\boldsymbol{j_u}$ depend on the active biomass. The term j_u in Eq. (11) applies across the stagnant liquid layer and the entire biofilm depth.

1.4. Biofilm zone mass balance

The flow of dissolved species across the biofilm layer was expected to decrease over time due to the thickness of the mass transfer boundary layer by reduced uranium precipitate. Therefore, as a result of these the transport of dissolved uranium species through the surface of the biofilm attached to the support media over time was based on molecular diffusion which follows Fick's law as follows:

$$j_u = D_{uw}\frac{dU_f}{dz} at 0 < z < L \quad (12)$$

A mass balance of the dissolved species over an infinitesimal film segment δz gives:

$$\frac{d}{dz}j_u = r_{uf} \quad (13)$$

Therefore, the partial differential equation (PDE) describing molecular diffusion of a particulate matter in water inside the biofilm is represented as follows:

$$-\frac{dU_f}{dt} = \frac{d}{dz} j_u + r_u f \tag{14}$$

$$-\frac{dU_f}{dt} = \frac{d}{dz}\left(D_{uw}\frac{dU_f}{dz}\right) + r_{uf} \tag{15}$$

Because the diffusion of species in the biofilm is influenced by the volume fraction (porosity) the diffusion-reaction biofilm equation for U(VI) removal rate and biomass growth rate within the biofilm is computed as a function of porosity as follows:

$$\varepsilon\frac{dU_f}{dt} = \varepsilon D_{uw}\frac{d^2U_f}{dz^2} + r_{uf} \tag{16}$$

$$\frac{dU_f}{dt} = \frac{dj_u}{dz} + \frac{r_{uf}}{\varepsilon} \tag{17}$$

where: $j_u = D_{uw}(dU/dz)$ flux rate of dissolved species ($ML^{-2}T^{-1}$), r_{uf} = removal rate of dissolve uranium species in the biofilm ($ML^{-3}T^{-1}$), δz = infinitesimal region across the biofilm (L), ε= biofilm porosity constant. The boundary conditions for dissolved species at the liquid-biofilm interface are defined as:

$$j_u = K_{LU}(U_B(t) - U_{f,s}(t, L_f)) \text{at} z = L_f [\text{innerboundary}] \tag{18}$$

j_u = 0 at z = 0 [outer boundary] (19)

2. Materials and methods

2.1. Culture and media

U(VI) reducing bacteria was isolated from soil samples collected from tailing dumps of an abandoned uranium mine in Pharaborwa (Limpopo Province, South Africa). Background uranium concentration in the original samples was detected at levels as high as 29 mg/kg much higher than values observed in natural soils (0.3–11.7 mg/kg) [27]. The isolated microorganisms from the above medium were therefore expected to be tolerant to high uranium concentration due to the high uranium background exposure conditions. Crumbs of sludge (2 g or less) were used to inoculate sterile Luria-Bettani (LB) broth and Nutrient broth (NB) to grow as many species as possible from the sludge. U(VI) resistant species were selected by spiking the nutrient rich broth with 75 mg/L U(VI). The cultures were plated on LB agar and pure colonies formed were sent for genetic analysis for species identification.

Pure culture isolates of U(VI) tolerant species were cultured in sterile basal mineral medium (BMM) consisting of: 10 mM NH_4Cl, 30 mM Na_2HPO_4, 20 mM KH_2PO_4, 0.8 mM Na_2SO_4, 0.2 mM $MgSO_4$, 50 µM $CaCl_2$, 0.1 µM $ZnCl_2$, 0.2 µM $CuCl_2$, 0.1 µM NaBr, 0.05 µM Na_2MoO_2, 0.1 µM $MnCl_2$, 0.1 µM KI, 0.2 µM H_3BO_3, 0.1 µM $CoCl_2$, and 0.1 µM $NiCl_2$ and D-glucose as the sole added carbon source. The medium was sterilized by autoclaving at 121 °C (2.5 bar) for 15 min prior to use. The sealed vessel containing BMM and inoculated cells was purged with 99.9% N_2 gas followed by incubation in a controlled temperature room at 30 ± 2 °C for 24 h.

After incubation for 24 h, pure cultures were isolated by plating serially diluted suspended cultures in 0.85% NaCl to achieve growth of separate colonies [28]. Individual colonies were streaked onto Luria-Bettani agar plates which were used as stock cultures for long-term storage.

2.2. Culture characterization

The sealed vessels inoculated with individual colony picks were purged with 99.9% pure N_2 gas followed for incubation for a period of 14 h at 30 ± 1 °C. Genomic DNA was extracted from the biomass grown from pure colonies following the protocol described for the Wizard Genomic DNA purification kit (Promega Corporation, Madison, WI, USA). 16S rRNA genes were then amplified by using a reverse transcriptase-polymerase chain reaction (RT-PCR) using primers pA and pH1 (Primer pA corresponds to position 8–27; Primer pH to position 1541-1522 of the 16S gene under the following reaction conditions: 1 min at 94 °C, 30 cycles of 30 s at 94 °C, 1 min at 50 °C and 2 min at 72 °C, and a final extension step of 10 min at 72 °C). PCR fragments were then cloned into pGEM-T-easy (Promega) [Promega Wizard® Genomic DNA Purification Kit (Version 12/2010)]. The 16S rRNA gene sequences of the strains were aligned with reference sequences from *Desulfovibrio* spp., *Geobacter* spp., *Acinetobacter* sand *Shewanella putrefaciens* using Ribosomal Database Project II programs. Sequence alignment was verified manually using the program BIOEDIT. Pairwise evolutionary distances based on an unambiguous stretch of 1274 bp were computed by using [29] method. The DNA sequence for each pure colony was then uploaded to the Basic Local Alignment Search Tool (BLAST) of the National Center for Biotechnology Information (NCBI). A phylogenetic tree was constructed from the identified 16S rRNA sequences using the neighbour-joining method in the MEGA Version 6 software [30].

2.3. Reactor set-up

The packed-bed column to be used as the fixed-film bioreactor was constructed from Plexiglas (PVC glass) tubes (1 m long, 0.1 m internal diameter). The column consisted of influent and effluent ports, and four equally spaced intermediate sampling ports with bed heights of (0.2 m, 0.4 m, 0.6 m, and 0.8 m). The column was packed with approximately 1.404 kg plastic media obtained from Happykoi (South Africa) with a nominal surface area of 0.235 m^2/kg (a total of 0.3298 m^2 per column). The columns were operated under fully submerged conditions with the recirculation stream fed from the bottom of the reactor. Provision was made for biomass analysis through sealable holes on PVC caps placed on the top end of the column. The packed column was installed vertically in a room with temperature set at 30 ± 2 °C (Fig. 1). The reactor and connecting tubes were autoclaved at 121 °C for 30 min prior to installation. The pore volume which represents the total reaction volume was determined from the difference between the weight of the saturated column with packing material and the weight of a dry fully packed column using the density of water occupying the pore spaces, ρ_w at 30 °C, as 0.98 g/cm^2. The specifications of the biofilm reactor are summarized in Table 1.

Table 1. Biofilm Reactor Specifications.

Column and packing material properties	Value
Height of the column	1 m
Diameter of column	0.1 m
Total volume of reactor	7.85 L
Total surface area of column	0.3298 m^2
Particle size	0.013 m × 0.01 m
Specific surface area	650 m^2/m^3
Density	0.179 kg/L
Packing Weight in the column	1.404 kg
Porosity	95%

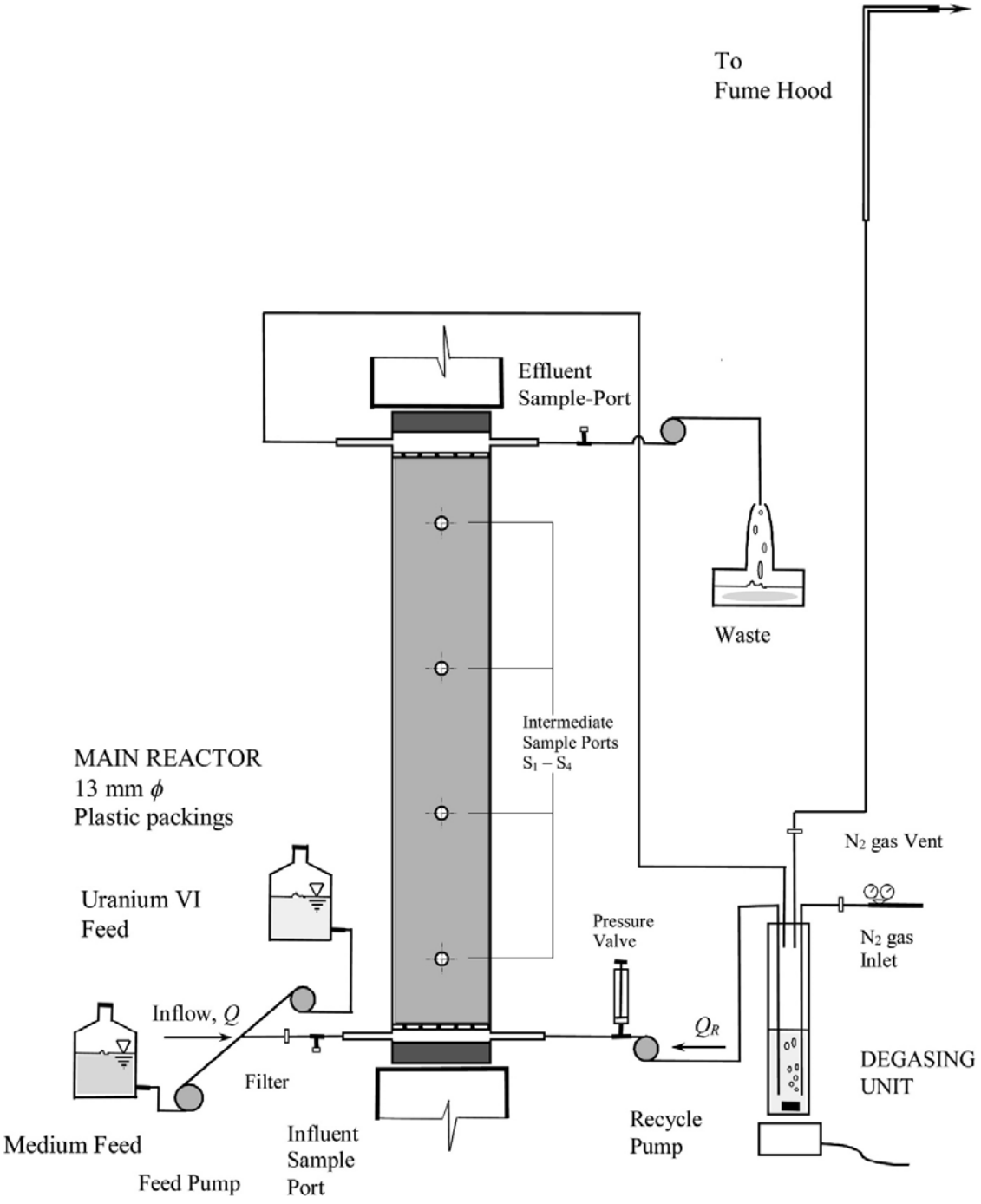

Fig. 1. Schematic of the packed-bed bioreactor operated anaerobically under oxygen stressed conditions and continuously mixed by the recirculation at $Q_R/Q \geq 20$.

2.4. Reactor start up

The reactor was seeded with 8 L suspended cells with a viable concentration of approximately 10^8 cells/mL. The above batch of viable cells was harvested at log-growth phase from LB and NB broth growth vessels. The harvested cells were re-suspended in sterile BMM amended with D-glucose as carbon and energy source. The viable cell solution was fed into the reactor in batch mode with 100% recirculation using a pre-calibrated peristaltic pump. The reactor was operated in the batch mode until biofilm was visible on the surfaces of the reactor packings.

2.5. Reactor operation

Biofilm reactors were operated at 24 h HRT which was later decreased to 12 and 8 h by increasing the flow rate. During the experimental run, sterile BMM amended with D-glucose and U(VI) solution of specific or target concentration ranging from (75–100 mg/L) was fed into the columns using pre-calibrated Masterflex peristaltic pumps (Cole-Palmer Inst. Co., Niles, Illinois). The columns were kept anaerobic mainly by operating under sealed conditions and by oxygen demand created by the organic substrate (D-glucose). The oxidation reduction potential (ORP) and the pH of the solution was measured continuously using ORP and pH probe (pHC101, MTC101, Hach, USA). The experiments were conducted at 30 ± 2 °C. Samples were withdrawn from the effluent port for U(VI) analysis.

2.6. Analytical methods

2.6.1. Determination of U(VI)

U(VI) reduction rate was determined by measuring the decrease in U(VI) in the solution using UV/Vis spectrophotometer (WPA, Light Wave II, and Labotech, South Africa). Arsenazo III (1,8-dihydroxynaphthalene-3,6 disulphonic acid-2,7-bis [(azo-2)-phenylarsonic acid]), a non-specific chromogenic reagent, was selected as the complexing agent for facilitating U(VI) detection [31]. Measurement of U(VI) was carried out by sampling 2 mL of solution from each sampling port in the reactors using disposable syringes. The withdrawn samples were then centrifuged at 6000 rpm (2820 *g*) for 10 min using Minispin-Microcentrifuge (Eppendorf, Hamburg, Germany). The centrifuged sample (0.5–1 mL) was then diluted with 0.4 mL of 2.5% diethylene-triaminepenta acetic acid (DTPA) and then diluted up to mark with BMM in a 10 mL volumetric flask. The homogenous solution was then mixed with 2 mL of complexing reagent (Arsenazo III) and was allowed to stand for full colour development prior analysis for U(VI) at a wavelength of 651 nm., The complexing reagent Arsenazo-III changed from

reddish-pink to shades of blue colour in the presence of U(VI). DTPA was added to mask the interference caused by other cations in solution [32].

2.6.2. Determination of total uranium

The unfiltered sample (0.5 mL) was withdrawn from the reactor for total uranium measurement. The sample was digested with 1 mL of 2 M HNO_3 and was allowed to stand for about 5 min to achieve complete reaction before analysis. To separate the biomass from uranium species, the digested sample was centrifuged for 10 min at 6000 rpm (2820 *g*). The reacted sample was then filtered through a 0.22 µm filter membrane to remove any remaining particles. The filtrate was collected and diluted up to mark with distilled water. Total uranium was then measured using Inductively-Coupled Plasma–Mass Spectrometry (ICP-MS) which was previously calibrated against the uranium atomic adsorption standard solution following the method previously developed by Chabalala and Chirwa [33].

2.6.3. Scanning Electron Microscopy (SEM)

Surface morphology of the biofilm and culture was evaluated using Scanning Electron Microscopy (SEM) (Joel, JSM-5800LV, Pleasanton, CA). The cells attached to the support material were washed in a phosphate buffer prior to dehydrating in a series of ethanol solutions (30%, 50%, 70%, 80%, and 90%) [34]. The biofilm on the support material was fixed in a 2.5% glutaraldehyde in 0.1 M phosphate buffer (pH 7.0) solution [35]. Samples were dried in liquid CO_2 and mounted on stubs with double-sided tape, coated with gold, and then observed under SEM.

2.6.4. Transmission Electron microscopy (TEM) and X-ray powder diffraction (XRD)

Samples were prepared for Transmission Electron Microscope (TEM) by fixation with 1–2% glutaraldehyde followed by dehydration and embedding in pure Quetol epoxy resin [35]. The precipitates generated within the bioreactor were also analyzed using Transmission Electron Microscope—Energy Dispersive X-ray spectrometer (TEM-EDX) (Joel JEM-2100 F, Joel, Tokyo, Japan) and X-ray Powder Diffraction (XRD). Samples for TEM analysis were initially dried at 60 °C and used for XRD using Bruker powder diffraction meter (Model D8 Advanced) with Cu-Kα radiation. The diffraction pattern was recorded from 8-84° (2θ) with a step size of 0.04° and the time per step size of 8.1 s. The chemical nature of uranium crystals was determined by comparison with the powder diffraction standard files in the 2007 PDF-2 database.

2.6.5. Evaluation of biomass

Packing media samples for viable cell analysis were taken from the columns using sterile tweezers. The sampled packings were initially weighed and then placed into a 9 mL sterile buffered Ringer's solution which was prepared by dissolving 2 Ringer's tablets into 1 L distilled water as per manufacture instruction (Merck, Johannesburg, South Africa). The packing material was washed thoroughly by agitation in 0.85% NaCl solution for three cycles or until adequate detachment of attached biomass from the packing media was achieved. The washing solution was then serially diluted and 1.0 mL of contents of each test tube was platted on nutrient agar and Luria-Bettani agar to determine cell count [20]. The plates were then incubated for 48 h at 30 ± 2 °C. The number of colonies were then counted and multiplied by a dilution factor. The bacterial count was reported as colony forming units (CFU) per mL of sample. A conversion factor of 1.766×10^{-10} mg/cell was determined (with $R^2 = 0.998$) using the method previously derived by Molokwane et al. [36]. The inactivated mass concentration of viable cells was used to determine the U(VI) reduction capacity (T_c) of the cells.

2.7. Electron donor stoichiometry

Cumulative U(VI) reduction analyses was assessed in continuous flow fixed-bed reactor to establish whether the microorganisms had reached their maximum ability to reduce U(VI) in the system. An example of a balanced stoichiometric relationship during U(VI) reduction using lactate as an electron donor is represented as follows:

$$UO_2^{2+} + 0.5CH_3CH_2OO^- + 0.5H_2O \xrightarrow{URB} UO_2 + 0.5CH_3COO^- + 0.5CO_2 + 2H^+ \quad (20)$$

The stoichiometric relation for U(VI) reduction in batch reactor using glucose as carbon source is represented by Eq. 21 with a net Gibbs Energy yield of approximately, $\Delta G^{o\prime} = -196$ kJ/e-mole.

$$C_6H_{12}O_6 + 9UO_2{}^{2+} + 6H \rightarrow 9U_4{}^{+} + 6HCO_3{}^{-} + 6H_2O \quad (21)$$

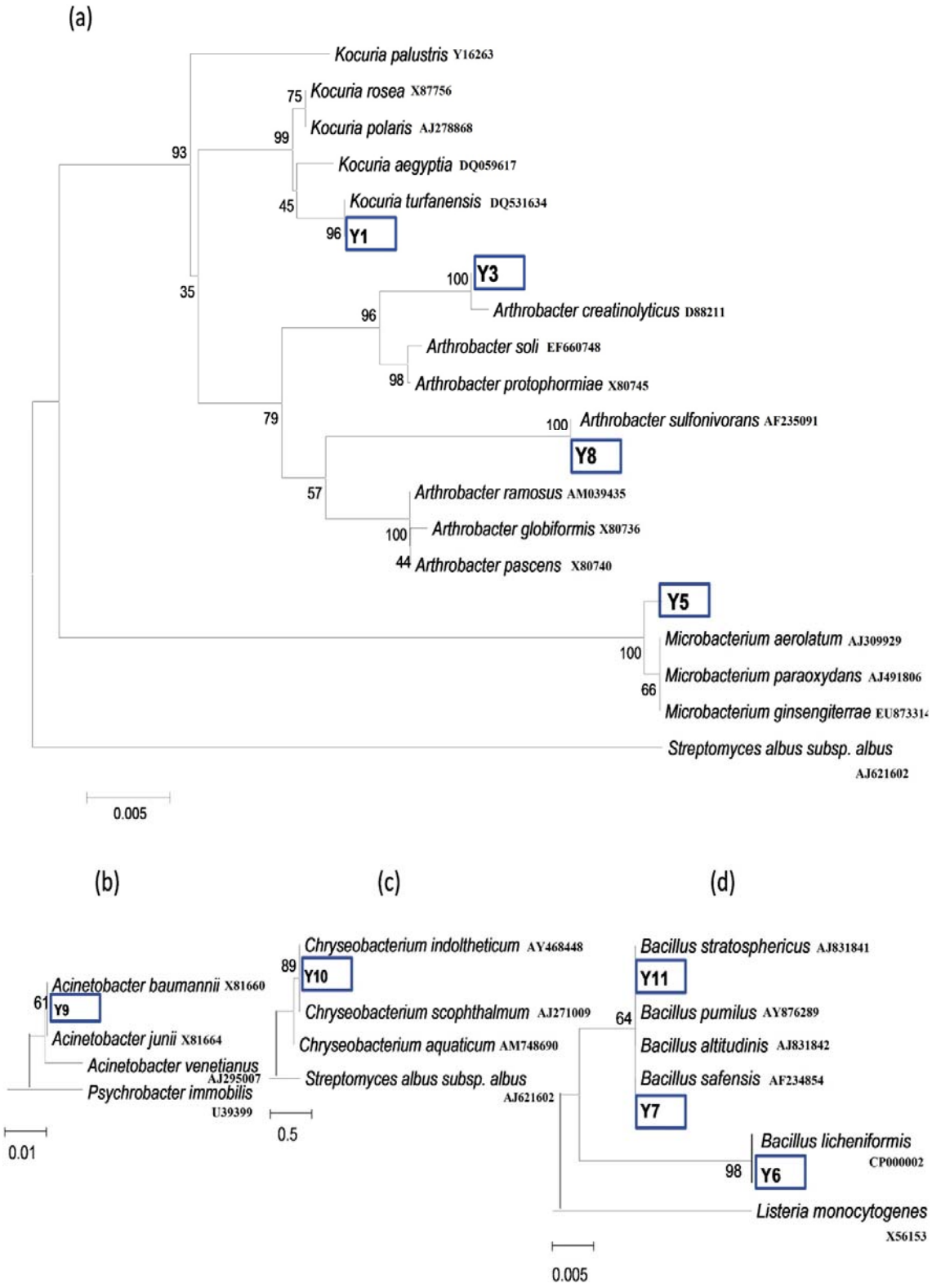

Fig. 2. Phylogenetic tree diagram developed from the BLAST search of the 16S rRNA genes of Gram (+ve) cells and Gram (–ve) cells from the original inoculum cultures from the mine tailing dump site in Phalaborwa (South Africa).

3. Results and discussion

3.1. Microbial screening and characterisation

The culture grown under U(VI) exposure of 75 mg U(VI)/L produced nine dominant colony phenotypes on Lurria-Bettani and Nutrient agar. The identified colonies were picked by sterile loop and transferred to different vessels with sterile media from which cells were harvested for DNA extraction and 16S rRNA characterisation as described earlier in Section 2.2. Phylogenetic analysis based on sequence identification of 16S rRNA genes showed that the isolates were members of genus *Bacillus*, *Microbacterium*, *Arthrobacter*, *Kocuria*, *Acinetobacter*, and *Chryseobacterium* as shown in Fig. 2. Among these candidates were species that have been previously reported by several researchers as being capable of reducing U(VI) to U(IV) [[37], [38], [39]]. Results from preliminary batch studies showed that, among the nine isolates shown in Fig. 2, Kocuria turfanensis, Arthrobacter creatinolyticus, *Bacillus licheniformis*, and *Microbacterium aerolatum* showed high U(VI) reducing capability under U(VI) dose of 75 mg/L. However, only *Bacillus licheniformis* among the suggested U(VI) reducers survived after day 99 of operation. The other species that survived from the original culture, *Acinetobacter baumanni*, is a well known Cr(VI) reducer. It is therefore possible that *Bacillus lichenoformis* and *Acinetobacter baumanni* were the main active U(VI) reducers in this culture. In a confirmatory test, batches inoculated with pure isolates of *Bacillus lichenoformis* achieved 93% U(VI) reduction in 75 mg/L U(VI) batches (Fig. 3). We can therefore conclude that the continued removal of U(VI) in the reactor was due to the persistent presence of *Bacillus lichenoformis*.

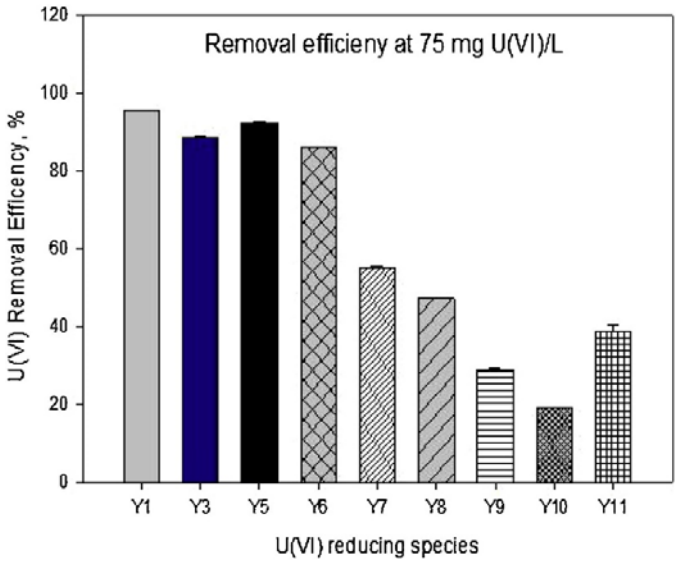

Fig. 3. U(VI) reduction in anaerobic batches at the initial U(VI) concentration of 75 mg/L.

3.2. Continuous-flow reactor performance

Abiotic U(VI) reduction in the biofilm reactor was ruled out using a cell-free (control) column with U(VI) feed at 75, 85 and 100 mg U(VI)/L. It was observed that the effluent U(VI) concentration in the cell-free reactor increased to the influent level over time (Fig. 4). The exponential rise of effluent U(VI) concentration observed in the clean packed-bed reactor without mixed-culture was consistent with a tracer response in a packed-bed reactor with no conversion, operated at a high recirculation rate (Q_R/Q_{in} = 20) to simulate CSTR conditions [40]. Effluent concentration in the presence of biomass was consistently lower than the U(VI) feed concentration under similar loading conditions. The improved U(VI) removal rates observed at the loading treatment of 85 mg/L may be attributed to the improvement of the biofilm system over time when certain favorable conditions were sustained. U(VI) removal efficiency of up to 98 ± 2% at the loading treatment of 85 mg/L was achieved.

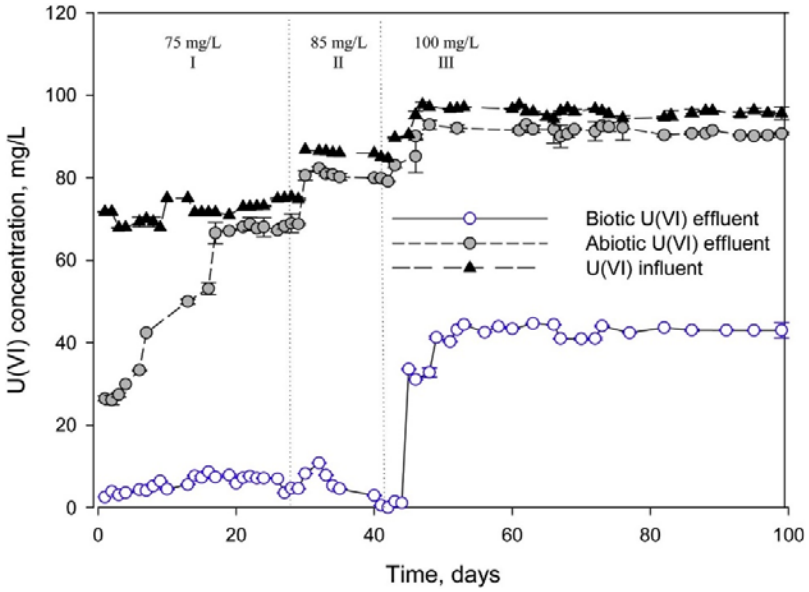

Fig. 4. Performance of biofilm reactor showing lack of removal of U(VI) in abiotic runs and up to 98% U(VI) removal in biotic runs.

Further increase of U(VI) feed concentration up to 100 mg/L resulted in decreased U(VI) removal efficiency. U(VI) removal efficiency of up to 60% was achieved at the loading treatment of 100 mg/L. The reduced U(VI) removal rate achieved at the loading treatment of 100 mg/L after 42 days of column operation was associated with the formation of the precipitate onto the biofilm layer which resulted in increased mass transfer resistance across the biofilm layer. These findings demonstrate the significance of metal-cell interactions within the biofilm matrix. U(IV) in the system was evaluated as the difference between total uranium

in the effluent and the remaining U(VI) in the effluent (Table 2). The assumption of biological U(VI) reduction to U(IV) in the system was confirmed by high total uranium concentration in the effluent as compared to U(VI) concentration measured in the effluent. However, relatively low total uranium concentration measured at the end of each phase in particular phase II and phase III (Table 2) suggests that most of the reduced uranium species were trapped on the packing media.

Table 2. Summary of total uranium (TU) and U(IV) after exposure to various U(VI) concentrations.

Phase	Influent U(VI) concentration (mg/L)	U(VI) loading rate ($g/m^3.d$)	Effluent[a] U(VI) (mg/L)	Total Uranium (TU)[b] (mg/L)	Effluent U(IV)[c] (mg/L)	Average U(VI) Removal [a](%)
I	75 ± 3	0.54	4.6	50.8 ± 3	45.4 ± 0.8	95 ± 2
II	85 ± 1.5	0.61	1.4	29.04 ± 1.2	27.64 ± 1.2	98 ± 2
III	100 ± 2.5	0.72	40	44.68 ± 0.4	4.68 ± 0.4	60 ± 1.7

a

value taken at the end of phase on the last effluent port.

b

value measured by the digestion method.

c

value calculated from TU-effluent U(VI).

3.3. Efficiency of U(VI) conversion – mass balance analysis

Fig. 5(a) shows that U(VI) removal increased continuously without signs of system failure under initial U(VI) concentration at 100 mg/L. The high cumulative U(VI) removal was due to the presence of U(VI) reducing bacteria and sufficient donor (5 g/L glucose) in system. The slope of cumulative U(VI) removal in a cell-free (control) reactor approached zero, demonstrating negligible U(VI) reduction over time.

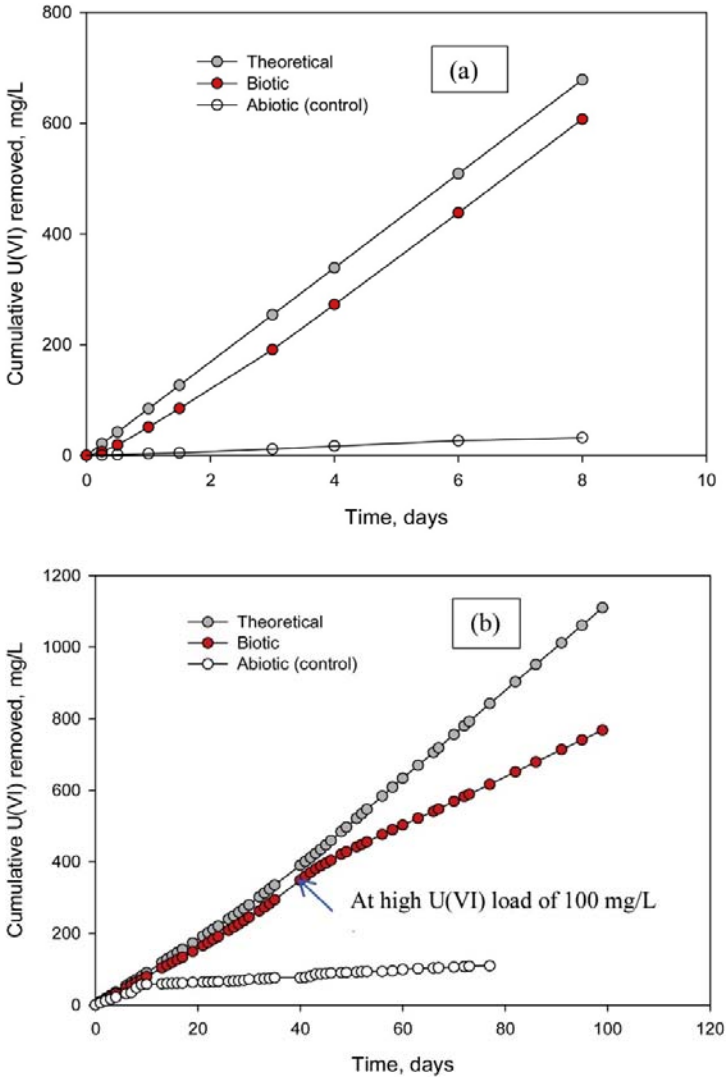

Fig. 5. Cumulative U(VI) removal by anaerobic culture isolates in (a) batch systems and (b) continuous flow bioreactor.

Similar to batch studies, data in Fig. 5(b) shows continuous increase in cumulative U(VI) removal slope in a biofilm reactor over time. The slope shows near perfect balance between theoretical and biotic cumulative U(VI) removal during the first 42 days of biofilm operation. U(VI) breakthrough occurred after 42 days when the bioreactor was operated at high U(VI) concentration of 100 mg/L. Moreover, the results in Fig. 5(b) also showed that the cumulative U(VI) removal at high influent U(VI) concentration of 100 mg/L remained high until the experiment was terminated. This indicates that the microbes were still able to reduce U(VI). The U(VI) reduction capacity observed at this point could be lost mainly due to accumulation of precipitate in the biofilm reactor which resulted to mass transfer resistance across the biofilm layer. Insignificant cumulative U(VI) removal was observed in the abiotic reactor.

3.4. Biomass analysis

The growth curve in Fig. 6 shows low viable attached biomass within the first 7 days of column operation at higher initial U(VI) concentration. The biomass population increased exponentially after 15 days of operation. After about 18 days of operation, the biofilm was assumed to have reached the mature stage. The increase in viable attached biomass population between 15 and 42 days suggests that the cells in the biofilm had acclimated to U(VI) exposure during this period. The decline in biomass concentration observed between 50 and 80 days was attributed to the toxicity effects on the microbial culture after operation under U(VI) overloaded conditions for a prolonged time.

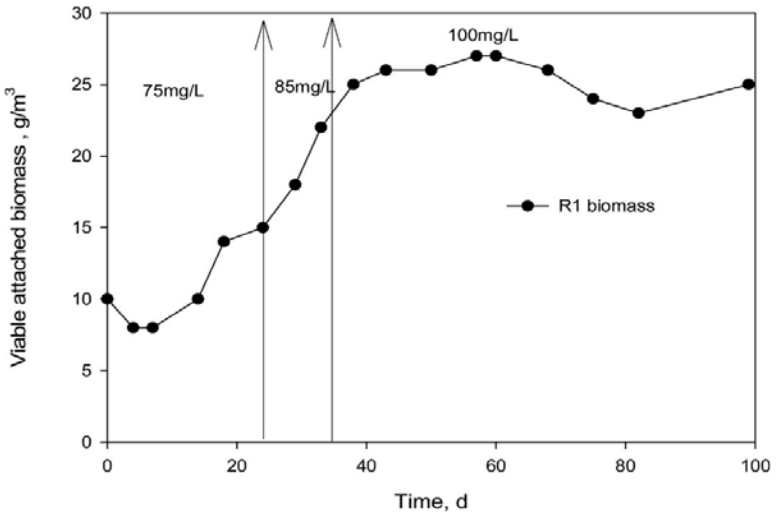

Fig. 6. Biomass growth rate in the continuous flow fixed-film bioreactor system.

3.5. Cellular localisation of reduced species

Uraninite deposits localization has been reported by researchers studying uptake and distribution of uranium deposits in Microbacterium, Arthrobacter, Bacilli, and several other uranium reducing bacterial species [[41], [42], [43]]. For example, Suzuki and Banfield [43] observed the intracellular accumulation of uranium in *Arthrobacter s*The precipitation of the uranium species inside the cells was localised around polyphosphate granules as (UO_2^{2+})-phosphate complexes demonstrating the involvement of phosphate group in uranium removal from solution. Fowle and co-workers [44] intensively studied adsorption of uranyl and aqueous uranyl complexes by functional groups of the bacterial cell wall of *Bacillus subtilis*. Recent studies by Sowmya et al. [45,46] demonstrated the effectiveness of *Acinetobacter s*(phosphate solubilizing bacteria) in immobilizing U(VI) in contaminated environments. In this study positive correlation (R^2 = 98%)

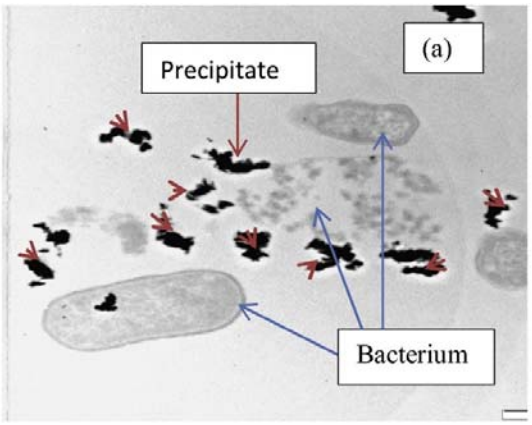
Precipitate
(a)
Bacterium

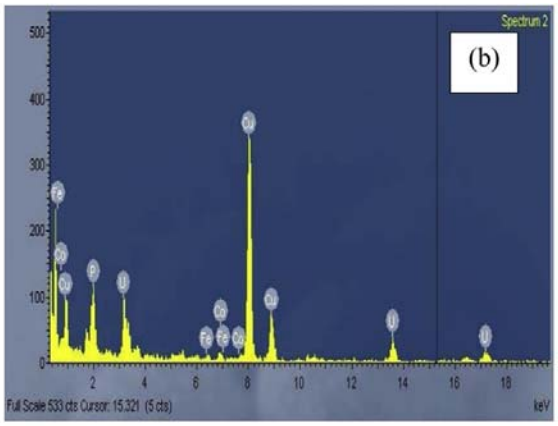
Spectrum 2
(b)
Full Scale 533 cts Cursor: 15.321 (5 cts)
keV

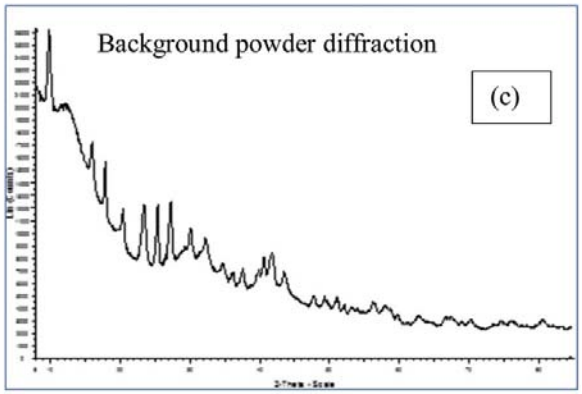
Background powder diffraction
(c)

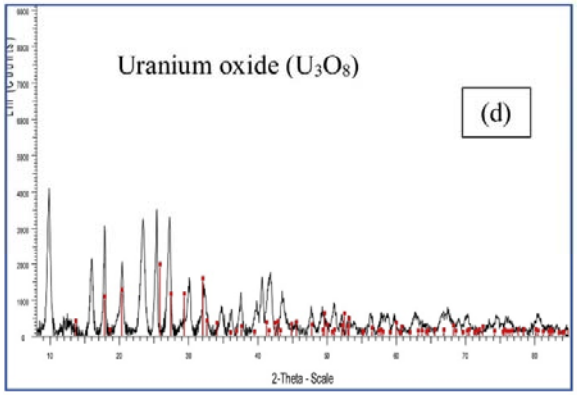
Uranium oxide (U_3O_8)
(d)
2-Theta - Scale

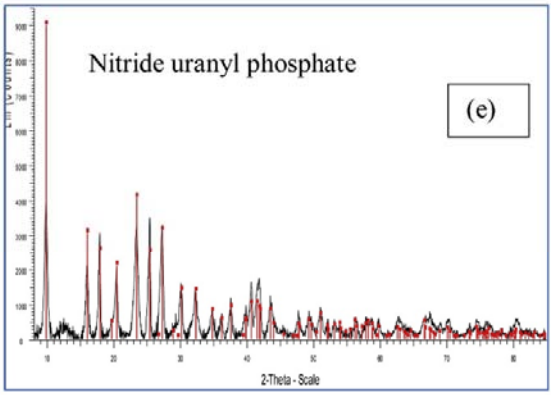
Nitride uranyl phosphate
(e)
2-Theta - Scale

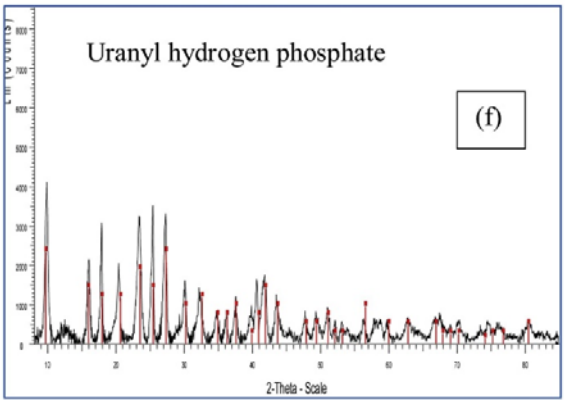
Uranyl hydrogen phosphate
(f)
2-Theta - Scale

Fig. 7. (a) TEM micrograph showing uranium deposits (indicated by arrows) on the cell surface (b) EDX spectra showing the presence of uranium, phosphate, and calcium in the precipitate. X-ray powder diffraction spectra of the reduced uranyl nitrate precipitate (c) before overlaying with reference database stick patterns, after overlaying with stick patterns of (d) U_3O_8, (e) deuterium nitride uranyl phosphate and (f) uranyl hydrogen phosphate hydrate. The reference database (vertical lines) shows good correlation with the reduced uranyl nitrate precipitate.

was observed between % decrease in phosphate and U(VI) concentration. These results were in agreement with literature results on similar cultures such as the *Kocuria s*by El-Sharouny et al. [47] in which uptake of U(VI) ions was determined to be through cell-surface biosorption. In the above study by El-Sharouny et al. [47] and Gholami et al. [48] *Kocuria spp* was reported to be tolerant to radiation.

In this study, the brownish precipitate formed onto the biofilm matrix in the bioreactor was characterized using TEM-EDX and X-Ray Diffraction (XRD) spectroscopy (Fig. 7). TEM-EDX showed the precipitate constituents of the following elements (U, Cu, P, Ca, Co, Fe). The higher copper (Cu) peaks observed was associated with the bleeding of the copper specimen support grid during bombardment with electrons. Results on XRD analysis showed that the precipitate was mainly composed of uranium oxide as (U_3O_8) and uranium phosphate compounds such as nitride uranyl phosphate. The presence of U_3O_8 demonstrate the presence of both U(VI) and U(IV) in the precipitate [49], while the presence of uranyl phosphate compounds confirms possible complexation of uranium with phosphate facilitating metal nucleation and bio-precipitation [[49], [50], [51]].

3.6. Superficial localisation of reduced uranium species

Scanning electron microscopy (SEM) was used to determine the surface morphology of the culture attached to the growth support medium. Scanning electron microscopy in Fig. 8b shows the evidence of biofilm formation onto the matrix prior feeding simulated U(VI) containing wastewater into the bioreactor. The phenomenon of elongated rod shape on anaerobically grown *Psedomonas aeruginosa* was also observed by Yoon and co-workers [52]. After operating the column for 99 days in the presence of U(VI), the biofilm formation onto the matrix was not observed (Fig. 8c). The unclear visibility of the biofilm after column operation was mainly due to deposition of uranium precipitate onto the matrix that accumulated over time.

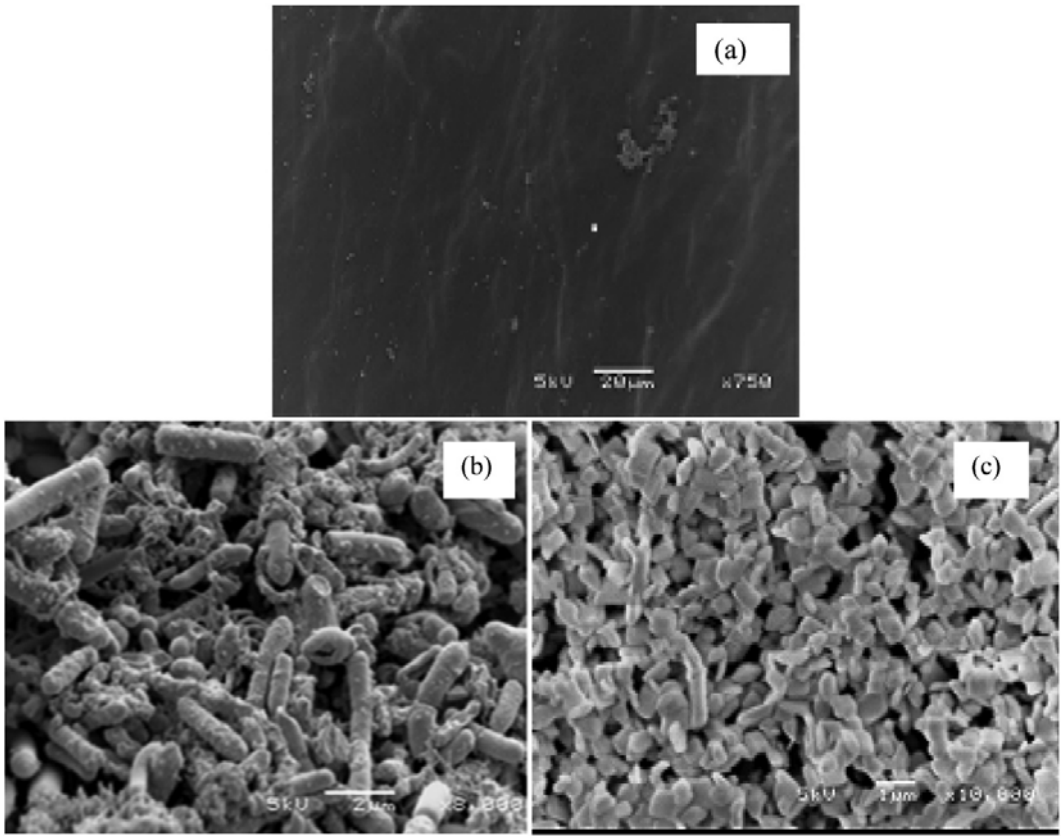

Fig. 8. SEM analyses of (a) cell-free media (b) after seeding the column with viable cell solution (c) after 99 days of biofilm exposure with various uranium concentrations.

3.7. Confirmation of U(VI) reducers in the reactor

As conditions in the reactor changed, i.e., change in Oxidation Reduction Potential (ORP) and establishment of biofilm, the culture composition changed significantly (Table 3). However, U(VI) reduction capacity of the culture was not lost. The two species that were detected in the original soil cultures and were not lost after operation of the reactor for 99 days were *Acinetobacter baumanni* and *Bacillus licheniformis*. Notably, several variants of *Acinetobacter spp* and *Bacillus lichenformis* have shown to be effect transitional metal reducers such Cr(VI) and Se(VI) [53]. For the above reason, these two species are suspected to be the ones responsible for U(VI) reduction in the reactor.

Table 3. Summary of microbial culture before and after operating the reactor for 99 days under various influent U(VI) concentrations.

Start-up Culture		Culture after 99 days of bioreactor operation
Kocuria turfanesis* belong to family *Micrococcaceae/Microbacterieceae		*Rhodococcus spp*, belonging to the family *Microbacterieceae*
Arthrobacter creatinolyticus		*Cellulosimicrobium spp*, belonging to the family *Microbacterieceae*
Microbacterium aerolatum*- belong to family *Microbacterieceae		*Curtobacterium spp*, belonging to the family *Microbacterieceae*
Bacillus licheniformis	→	*Bacillus spp*, possibly *Bacillus licheniformis/ altitudinis*
Acinetobacter baumanni	→	*Acinetobacter baumanni*

4. Conclusion

Continuous-flow bioreactor systems have the potential of treating U(VI) concentrations at much higher volumes. The results from this study showed the ability of the fixed-bed biofilm reactor in sustaining high U(VI) concentrations of up to 85 mg/L under oxygen stressed conditions without the addition of any external organic carbon source. U(VI) was removed effectively until a higher concentration of 100 mg U(VI)/L were removal efficiency decreased to 60%. The potential of the indigenous isolates of bacteria grown as a biofilm in reducing or stabilizing U(VI) under various feed of U(VI) conditions was successfully demonstrated. U(VI) removal achieved in the fixed-bed biofilm system which was operated addition of external organic carbon source was associated both to effectiveness of the indigenous mixed-culture and the interrelationships that occur within the heterogeneous biofilm structure. Although, results presented in this study have strong implications of biological U(VI) reduction *ex-situ* through the use of the bioreactor system, these results could also be effective in optimizing and improving the operation and performance of *in situ* bioremediation of U(VI) at contaminated sites. Further studies are required to investigate U(VI) reduction recovery in the biofilm reactor by removing the trapped uranium precipitated through backwashing or by agitating the system with a high flow of nitrogen. This will not only improve the performance of the biofilm system in U(VI) removal process, but also provide an opportunity to recover uranium and phosphate for beneficial use.

Acknowledgements

The research was funded by South Africa's National Research Foundation (NRF) through the Competitive Programme for Rated Researchers Grant No. CPR20110603000019146 and the Incentive Funding for Rated Researchers (IFRR) Grant No. IFR2010042900080 awarded to Evans M.N. Chirwa of the University of Pretoria. Additional financial support was received from Sasol South Africa (Pty) Ltd as supplementary research funds and a student bursary Grant No. PIF-Ref:525/08-14 awarded to Phalazane J. Mtimunye at the University of Pretoria.

References

[1] G. Hoppe, F. Damaschun, G. Wappler. An appreciation of Martin Heinrich Klaproth as a mineral chemist. Pharmazie, 42 (1987), pp. 266-267

[2] F. Gauthier-Lafaye, P. Holliger, P.-L. Blanc. Natural fission reactors in the Franceville Basin, Gabon: a review of the conditions and results of a "critical event" in a geologic system. Geochim. Cosmochim. Act., 60 (25) (1996), pp. 4831-4852

[3] O. Hahn, F. Strassmann. On the detection and characteristics of the alkaline earth metals formed by irradiation of uranium with neutrons. Über den Nachweis und das Verhalten der bei der Bestrahlung des Urans mittels Neutronen entstehenden Erdalkalimetalle. Die Naturwissenschaften, 27 (1939), pp. 11-15

[4] U. Amaldi, E. Fermi. His work and legacy. C. Bernardini, L. Bonolis (Eds.), Nuclear Physics from the Nineteen Thirties to the Present Day. Nuclear Physics from the Nineteen Thirties to the Present Day Nuclear Physics from the Nineteen Thirties to the Present Day Bologna, Springer, Società Italiana di Fisica (2001), pp. 151-176

[5] S.A. Qvist, B.W. Brook. Potential for worldwide displacement of fossil-fuel electricity by nuclear energy in three decades based on extrapolation of regional deployment data. PLoSONE (May) (2013), 10.1371/journal.pone.0124074

[6] J. Plant, P.R. Simpson, B. Smith, B.F. Windley. Uranium ore deposits: products of the radioactive earth. P.C. Burns, R. Finch (Eds.), Reviews in Mineralogy, Vol 38, Uranium: Mineralogy, Geochemistry and the

Environment, Mineralogical Society of America, Washington D.C., U.S.A (1999), pp. 255-320

[7] T.G. Korzpn, T.K. Kyser. O, U, and Pb isotopic and chemical variations in uraninite: implications for determining the temporal and fluid history of ancient terrains. Am. Mineral., 78 (1993), pp. 1262-1274

[8]P. Zhou, P. Gu. Extraction of oxidized and reduced forms of uranium from contaminated soils: effects of carbonate concentration and pH. Environ. Sci. Technol., 39 (2005), pp. 4435-4440

[9] D.A. Ross. Technical Report on the Patterson Lake South Property, Northern Saskatchewan, Canada, NI 43-101 Report. (2015) (Accessed 17, December 2017) http://www.fissionuranium.com/_resources/reports/RPA_Fission_U_Patterson_Lake_South_Technical_Report_FINAL_Feb_2015.pdf

[10] K.T. Thomas. Management of wastes from uranium mines and mills. IAEA Bull., 23 (2) (1981)

[11] H.S. Davies, F. Cox, C.H. Robinson, J.K. Pittman. Radioactivity and the environment: technical approaches to understand the role of arbuscular mycorrhizal plants in radionuclide bioaccumulation. Front. Plant Sci., 8 (2015), 10.3389/fpls.2015.00580. Art 580

[12] R.I. Bersimbaev, O. Bulgakova. The health effects of radon and uranium on the population of Kazakhstan. Genes Environ., 37 (18) (2015), 10.1186/s41021-015-0019-3

[13] M. Sutton, S.R. Burastero. Uranium(VI) solubility and speciation in simulated elemental human biological fluids. Chem. Res. Toxicol., 17 (2004), pp. 1468-1480

[14] S. Barillet, C. Adam, O. Pallue, A. Devaux. Bioaccumulation, oxidative stress, and neurotoxicity in *Danio rerio* exposed to different isotopic compositions of uranium. Environ. Toxicol. Chem., 26 (2007), pp. 497-505

[15] S. Chabalala, E.M.N. Chirwa. Uranium(VI) reduction and removal by high performing purified anaerobic cultures from mine soil. Chemosphere, 78 (2010), pp. 52-55

[16] S. Chabalala, E.M.N. Chirwa. Uranium (VI) reduction under facultative anaerobic conditions. Proc. 84th Annual Water Environment Federation Technical Exhibition and Conference (WEFTEC), Los Angeles (2011), pp. 6565-6573

[17] D.T. Reed, S.E. Pepper, M.K. Richmann, G. Smith, R. Deo, B.E. Rittmann. Subsurface bio-mediated reduction of higher valent uranium and plutonium. J. Alloys Comp. 444-445 (2007), pp. 376-382

[18] L. Semprini, P.L. McCarty. Comparison between model simulations and field results for in-situ biorestoration of chlorinated aliphatics: part 1. Ground Water, 29 (1981), pp. 365-374

[19] H. Shen, Y.-T. Wang. Modeling hexavalent chromium reduction in *Escherichia coli* ATCC 33456. Biotechnol. Bioeng., 43 (1994), pp. 293-300

[20] T. Srinath, T. Verma, P.W. Ramteke, S.K. Garg. Chromium (VI) biosorption and bioaccumulation by chromate resistant bacteria. Chemosphere, 48 (4) (2002), pp. 427-435

[21] S. Viamajala, B.M. Peyton, J.N. Petersen. Modeling chromate reduction in *Shewanella oneidensis* MR-1: development of a novel dual-enzyme kinetic model. Biotechnol. Bioeng., 83 (7) (2003), pp. 790-797

[22] C.K. Meli. Microbial Cr(VI) Reduction in Indigenous Cultures of Bacteria: Characterization and Modelling. Master of Science Dissertation University of Pretoria (2009). Last accessed, 21/12/2018 at 10:00 PM

http://repository.up.ac.za/bitstream/handle/2263/29842/dissertation.pdf;sequence=1

[23] P.E. Molokwane, E.M. Nkhalambayausi-Chirwa. Microbial culture dynamics and chromium (VI) removal in packed-column microcosm reactors. Water Sci. Technol., 60 (2) (2009), pp. 381-388

[24] J. Monod. The growth of bacterial cultures. Ann. Rev. Microbiol., 3 (1949), pp. 371-394

[25] E.M.N. Chirwa. Modeling Chromium(VI) Reduction in Pure and Coculture Biofilm Reactors. PhD Dissertation. Department of Civil Engineering, University of Kentucky, Lexington, Kentucky, USA (2000), p. 40506

[26] E.M. Nkhalambayausi-Chirwa, Y.-T. Wang. Modeling Cr(VI) reduction and phenol degradation in a coculture biofilm reactor, ASCE. J. Environ. Eng., 131 (11) (2005), pp. 1495-1506

[27] P.V. Tikilili, E.M.N. Chirwa. Characterization and biodegradation of polycyclic aromatic hydrocarbons in radioactive wastewater. J. Hazard. Mater., 192 (2011), pp. 1589-1596

[28] APHA. Standard Methods for the Examination of Water and Wastewater - Centennial Edition. American Public Health Association, American Water Works Association, Water Environment Federation, USA (2005)

[29] T.H. Jukes, C.R. Cantor. Evolution of protein molecules. H.N. Munro (Ed.), Mammalian Protein Metabolism., Academic Press, New York (1969), pp. 21-123

[30] K. Tamura, G. Stecher, D. Peterson, A. Filipski, S. Kumar. MEGA6: molecular evolutionary genetics analysis version 6.0. Mol. Biol. Evol., 30 (2013), pp. 2725-2729

[31] S.B. Savvin. Analytical use of arsenazo III: determination of thorium, zirconium, uranium and rare earth elements. Talanta, 8 (1961), pp. 673-685

[32] F.W.E. Strelow, T.N. Van Der Walt. Comparative study of the masking effect of various complexans in the spectrophotometric determination of uranium with arsenazo III and chlorophosphonazo III. Talanta, 26 (1979), pp. 537-542

[33] S. Chabalala, E.M.N. Chirwa. Removal of uranium(VI) under aerobic and anaerobic conditions using an indigenous mine consortium. Minerals Eng, 23 (6) (2010), pp. 526-531

[34] L. Goodridge, J. Chen, M. Griffiths. evelopment and characterization of a fluorescent-bacteriophage assay for detection of Escherichia coli O157:H7. Appl. Environ. Microbiol., 65 (1999), pp. 1397-1404

[35] A.M. Glauert. Fixation, dehydration and embedding of biological specimens. A.M. Glauert (Ed.), Practical Methods in Electron Microscopy., North-Holland Biomedical Press, Amsterdam (1975), pp. pp.1-201

[36] P.E. Molokwane, C.K. Meli, E.M. Nkhalambayausi-Chirwa. Chromium (VI) reduction in activated sludge bacteria exposed to high chromium loading: Brits culture (South Africa). Water Res., 42 (2008), pp. 4538-4548

[37] Y. Katsenovich, D. Carvajal, R. Guduru, L. Lagos, C.-Z. Li. Assessment of the resistance to uranium (VI) exposure by *Arthrobacter sp*. Isolated from Hanford site soil. Geomicrobiol. J., 30 (2013), pp. 120-130

[38] S.H. Thomas, E. Padilla-Crespo, P.M. Jardine, R.A. Sanford, F.E. Löffler. Diversity and distribution of Anaeromyxobacter strains in a uranium-contaminated subsurface environment with a nonuniform groundwater flow. Appl. Environ. Microbiol., 75 (2009), pp. 3679-3687

[39] C. Zhang, S.V. Malhotra, A.J. Francis. Toxicity of ionic liquids to *Clostridium sp*. And effects on uranium biosorption. J. Hazard. Mater., 264 (2014), pp. 246-253

[40] E.M. Nkhalambayausi-Chirwa, Y.-T. Wang. Simultaneous chromium(VI) reduction and phenol degradation in a fixed-film coculture bioreactor: reactor performance. Water Res., 35 (2001), pp. 1921-1932

[41] M. Nedelkova, M.L. Merroun, A. Rossberg, C. Hennig, S. Selenska-Pobell. Microbacterium isolates from the vicinity of a radioactive waste depository and their interactions with uranium. FEMS Microbiol. Ecol., 59 (2007), pp. 694-705

[42] L.M. Merroun, S. Selenska-Pobell. Bacterial interactions with uranium: an environmental perspective. J. Contam. Hydrol., 102 (2008), pp. 285-295

[43] Y. Suzuki, J. Banfield. Resistance to, and accumulation of, uranium by bacteria from a uranium-contaminated site. J. Geomicrobiol., 21 (2004), pp. 113-121

[44] D.A. Fowle, J.B. Fein, A.M. Martin. Experimental study of uranyl adsorption onto Bacillus subtilis. Environ. Sci. Technol., 34 (2000), pp. 3737-3741

[45] S. Sowya, P.D. Rekha, K. Naregundi, Y. Chiu-Chung, A.B. Arun. Phosphate solubilizing uranium tolerant bacteria associated with monazite sand natural background radiation site in South-West coast of India. Ann. Microbiol., 2014 (2014), 10.1007/s132113-014-0812-4

[46] S. Sowya, P.D. Rekha, A.B. Arun. Uranium(VI) bioprecipitation mediated by a phosphate solubilizing *Acinetobacter* sp. YU-SS-SB-29 isolated from high natural background site. Int. Biorem. Tech., 94 (2014), pp. 134-140

[47] E.E. El-Sharouny, M.A. Belal, H.H. Yusef. Isolation and characterization of two novel local psychrotolerant Kocuria sWith high affinity towards metal cations Biosorption. Life Sci. J., 10 (2013), pp. 1721-1737

[48] M. Gholami, Z. Etemadifar, M. Bouzari. Isolation a new strain of *Kocuria rosea* capable of tolerating extreme conditions. J. Env. Radioact., 144 (2015), pp. 113-119

[49] M. Martins, M.L. Faleiro, A.M. Rosa da Costa, S. Chaves, R. Tenreiro, A.P. Matos, M.C. Costa. Mechanism of U(VI) removal by two anaerobic bacterial communities. J. Hazard. Mater., 184 (2010), pp. 89-96

[50] S. Choudhary, P. Sar. Uranium biominerilization by resistant *Pseudomonas aeruginosa* strain isolated from contaminated mine waste. J. Hazard. Mater., 186 (2011), pp. 336-343

[51] S.K. Kazy, S.F. D'Souza, P. Sar. Uranium and Thorium sequestration by *Pseudomonas* sp.: mechanism and chemical characterization. J. Hazard. Mater., 163 (2009), pp. 65-72

[52] M.Y. Yoon, K. Lee, Y. Park, S.S. Yoo. Contribution of cell elongation to the biofilm formation of *Pseudomonas aeruginosa* during anaerobic respiration. PLoS One, 6 (2011), pp. 1-11

[53] Z.A. Zakaria, Z. Zakaria, S. Surif, W.A. Ahmad. Biological detoxification of Cr(VI) using wood-husk immobilized Acinetobacter haemolyticus. J. Hazard. Mater., 148 (1-2) (2007), pp. 164-171